JOURNAL OF ENZYME INHIBITION AND MEDICINAL CHEMISTRY, 2017
VOL. 32, NO. 1, 193–202
http://dx.doi.org/10.1080/14756366.2016.1247054

Taylor & Francis
Taylor & Francis Group

ORIGINAL ARTICLE

OPEN ACCESS

Novel 1-(2-pyrimidin-2-yl)piperazine derivatives as selective monoamine oxidase (MAO)-A inhibitors

Betül Kaya[a], Leyla Yurttaş[a], Begüm Nurpelin Sağlik[a,b], Serkan Levent[a,b], Yusuf Özkay[a,b] and Zafer Asim Kaplancikli[a]

[a]Department of Pharmaceutical Chemistry, Faculty of Pharmacy, Anadolu University, Eskişehir, Turkey; [b]Doping and Narcotic Compounds Analysis Laboratory, Faculty of Pharmacy, Anadolu University, Eskişehir, Turkey

ABSTRACT

In the present study, a new series of 2-[4-(pyrimidin-2-yl)piperazin-1-yl]-2-oxoethyl 4-substituted piperazine-1-carbodithioate derivatives (**2a-n**) were synthesized and screened for their monoamine oxidase A and B inhibitory activity. The structures of compounds were elucidated using spectroscopic methods and some physicochemical properties of new compounds were predicted using Molinspiration and MolSoft programs. Compounds 2-[4-(pyrimidin-2-yl)piperazin-1-yl]-2-oxoethyl 4-(4-nitrophenyl)piperazine-1-carbodithioate (**2j**) and 2-[4-(pyrimidin-2-yl)piperazin-1-yl]-2-oxoethyl 4-benzhydrylpiperazine-1-carbodithioate (**2m**) exhibited selective MAO-A inhibitory activity with $IC_{50} = 23.10$, 24.14 μM, respectively. Some of the biological results were found in accordance with the obtained *in silico* data based on Lipinski's fule of five.

ARTICLE HISTORY
Received 5 May 2016
Revised 3 August 2016
Accepted 3 October 2016

KEYWORDS
Depression; Lipinski's rule of five; Molinspiration; MolSoft; monoamine oxidase A; (2-pyrimidinyl)piperazine

Introduction

By definition depression means a serious and common disorder including symptoms like feeling of sadness, hopelessness, weight loss or gain, tiredness, changes in sleeping routine and thinking of suicide[1]. Depression is a major public health problem, and the fourth cause of the global burden of disease[2]. In the history of development of antidepressants, tricyclic antidepressants and monoamine oxidase inhibitors (MAOIs) were the first-generation antidepressants introduced in the late 1950s[3,4]. Selective serotonin reuptake inhibitors (SSRIs) noradrenaline reuptake inhibitors, serotonin–norepinephrine reuptake inhibitors (SNRIs) and dopamine–noradrenaline reuptake inhibitors (DNRIs) were improved as the new generation of antidepressants with fewer adverse effects than traditional antidepressants[5,6]. Despite many developments in the field of antidepressants, the clinical use of currently used drugs were restricted as a result of various adverse effects and a response in less than 50% of patients[7,8]. Thereby search for new class of antidepressant agents more effective, safe and with a more advantageous benefit–risk balance is an urgent need.

Aminergic neurotransmitters such as norepinephrine and serotonin (5-HT) became as key aspects in the therapy of depression. MAOIs are one of the most widely used groups of antidepressants agents regulating the metabolism of serotonin and norepinephrine. Monoamine oxidase enzymes (MAOs) control the concentration of neurotransmitters and intracellular amines in brain and peripheral tissues through catalyzing the oxidative deamination of them[9]. MAOs are localized in outer mitochondrial membrane's of neuronal, glial, and other cells and contain the covalently linked cofactor flavin adenine dinucleotide (FAD)[10]. MAO-A mostly select serotonin, adrenaline and noradrenaline as subtrate, whereas MAO-B metabolize phenylethylamine and benzylamine[11]. Besides, tyramine and dopamine were metabolized by both forms of the enzyme[12]. Two groups of MAO enzymes namely MAO-A and MAO-B were classified on the basis of their affinities to inhibitors, specificities to substrates and tissue/cellular distribution[13,14]. MAO-A inhibitors are clinically used in the treatment of depression and anxiety[15] while MAO-B inhibitors are mostly used in Parkinson's and Alzheimer's diseases[14].

The azapirones (buspirone, gepirone, ipsapirone, tandospirone and zalospirone, Figure 1) have been known to exhibit anxiolytic and antidepressant activities[16]. 1-(2-Pyrimidinyl)piperazinyl (1-PP) pharmacophore widely exists in the azapirones structure and it is an active metabolite of azapirones[17]. The most notable azapirone, buspirone, is a selective 5-HT1A agonist that is used clinically as an antidepressant drug[18–20]. In contrast to diazepam, buspirone does not cause sedation or muscle relaxation[21]. In a study, it was reported that the connection of 1-PP pharmacophores with appropriate side chains may eliminate neuroleptic-like side effects thus produce non-dopaminergic agents[22]. Furthermore, between 5-HT1A receptor ligands, long-chain arylpiperazines such as 1-PP comprise one of the most important classes[23]. Due to the fact that there are some studies support that compounds bearing 1-PP moiety possess antidepressant, anxiolytic and antipsychotic activity[16,22,24–26]. *In vivo* produced 1-PP moiety is estimated to be partly in charge of the efficacy of the azapirones in the therapy of depression[27,28]. Piperazine derivatives have been also known to exhibit antidepressant activity[29,30].

Based on these observations mentioned above, we report the synthesis and monoamine oxidase inhibitory activity of some novel 2-[4-(pyrimidin-2-yl)piperazin-1-yl]-2-oxo-ethyl 4-substituted piperazine-1-carbodithioate derivatives (**2a-n**) in the present study.

Materials and methods

Melting points were determined by MP90 digital melting point apparatus (Mettler Toledo, Columbus, OH) and were uncorrected. Spectroscopic data were recorded on the following instruments: a Bruker Tensor 27 IR spectrophotometer; a ^{1}H NMR (nuclear magnetic resonance) Bruker DPX-500 FT-NMR spectrometer, ^{13}C NMR,

CONTACT Leyla Yurttaş lyurttas@anadolu.edu.tr Department of Pharmaceutical Chemistry, Faculty of Pharmacy, Anadolu University, 26470 Eskisehir, Turkey

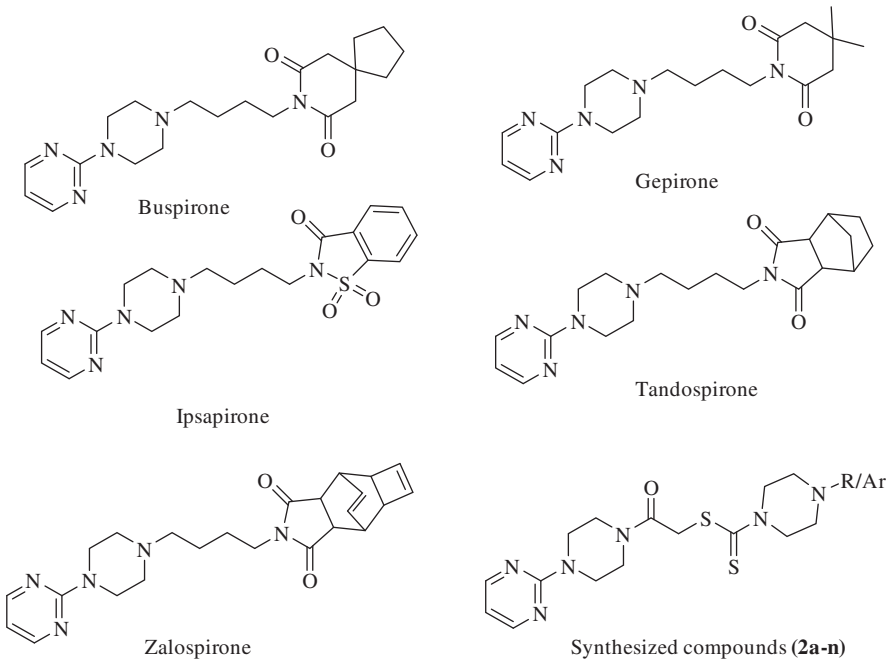

Figure 1. Structures of azopirones (buspirone, gepirone, ipsapirone, tandopirone and zalospirone) and general structrure of the synthesized compounds (**2a-n**).

Bruker DPX 125 MHz spectrometer (Bruker Bioscience, Billerica, MA); M + 1 peaks were determined by Shimadzu LC/MS ITTOF system (Shimadzu, Tokyo, Japan). Elemental analyses were performed in a Perkin Elmer EAL 240 elemental analyser for C, H and N.

General method for synthesis of 2-[4-(pyrimidin-2-yl)piperazin-1-yl]-2-oxoethyl 4-substituted piperazine-1-carbodithioate derivatives (2a-n)

A mixture of 2-chloro-*N*-[4-(2-pyrimidinyl)piperazine]acetamide and potassium salt of appropriate piperazine dithiocarbamate derivative (10 mmol) was stirred in acetone at room temperature with the presence of potassium carbonate (10 mmol). After the reaction finished, controlled with TLC, the reaction mixture was poured into ice-water and the precipitated portion was filtered and crystallised from ethanol to gain the final products.

2-[4-(Pyrimidin-2-yl)piperazin-1-yl]-2-oxoethyl 4-methylpiperazine-1-carbodithioate (2a)

Yield 71%, m.p. 145–150 °C. IR ν_{max}(cm^{-1}): 3066 (aromatic C–H), 2933 (aliphatic C–H), 1639 (amide C=O), 1581–1431 (C=C and C=N), 1286–1028 (C–N and C–O). ^{1}H-NMR (500 MHz, DMSO-d$_6$, ppm) δ 2.21 (s, 3H, CH_3), 2.41 (brs, 4H, piperazine), 3.55–3.73 (m, 8H, piperazine), 3.95 (brs, 2H, piperazine), 4.21 (brs, 2H, piperazine), 4.30 (s, 2H, CO-CH_2), 6.68 (t, 1H, J = 4.70 Hz, Ar-H), 8.40 (d, 2H, J = 4.8 Hz, Ar-H). ^{13}C-NMR (125 MHz, DMSO-d$_6$, ppm) δ 14.02, 29.27 (S-CH_2), 41.95, 43.49, 45.50, 51.43, 54.44, 70.84, 110.99 (pyrimidine C_5), 158.47 (pyrimidine C_4, C_6), 161.55 (pyrimidine C_2), 165.15 (C=O), 194.98 (C=S). For $C_{16}H_{24}N_6OS_2$ calculated: 50.50% C, 6.36% H, 22.09% N; found: 50.54% C, 6.42% H, 22.15% N. HRMS (*m/z*): $[M+H]^+$ calcd for $C_{16}H_{24}N_6OS_2$: 381.1526; found 381.1508.

2-[4-(Pyrimidin-2-yl)piperazin-1-yl]-2-oxoethyl 4-ethylpiperazine-1-carbodithioate (2b)

Yield 64%, m.p. 200–202 °C. IR ν_{max}(cm^{-1}): 3055 (aromatic C–H), 2968 (aliphatic C–H), 1641 (amide C=O), 1581–1431 (C=C and C=N), 1257–1028 (C–N and C–O). ^{1}H-NMR (500 MHz, DMSO-d$_6$, ppm) δ 1.03 (t, 3H, J = 7.15 Hz, $CH_2\underline{CH_3}$), 2.36–2.47 (m, 4H, $\underline{CH_2}CH_3$ and piperazine 2H), 3.55 (brs, 2H, piperazine), 3.67–3.70 (m, 4H, piperazine), 3.83 (brs, 2H, piperazine), 3.96 (brs, 2H, piperazine), 4.21 (brs, 4H, piperazine), 4.38 (s, 2H, CO-CH_2), 6.68 (t, 1H, J = 4.7 Hz, pyrimidine), 8.40 (d, 2H, J = 4.7 Hz, pyrimidine). ^{13}C-NMR (125 MHz, DMSO-d$_6$, ppm) δ 12.34, 29.56 (S-CH_2), 41.97, 43.55, 45.62, 51.49, 52.23, 110.97 (pyrimidine C_5), 158.46 (pyrimidine C_4, C_6), 161.39 (pyrimidine C_2), 165.77 (C=O), 194.29 (C=S). For $C_{17}H_{26}N_6OS_2$ calculated: 51.75% C, 6.64% H, 21.30% N; found: 51.64% C, 6.52% H, 21.16% N. HRMS (*m/z*): $[M+H]^+$ calcd for $C_{17}H_{26}N_6OS_2$: 395.1682; found 395.1668.

2-[4-(Pyrimidin-2-yl)piperazin-1-yl]-2-oxoethyl 4-(2-hydroxyethyl)piperazine-1-carbodithioate (2c)

Yield 66%, m.p. 199–202 °C. IR ν_{max}(cm^{-1}): 3495 (O-H), 3034 (aromatic C–H), 2940 (aliphatic C–H), 1633 (amide C=O), 1581–1435 (C=C and C=N), 1230–1153 (C–N and C–O). ^{1}H-NMR (500 MHz, DMSO-d$_6$, ppm) δ 2.44 (t, 2H, J = 6.0 Hz, N-CH_2), 2.53 (brs, 4H, piperazine), 3.51–3.54 (m, 4H, piperazine, CH_2OH), 3.66–3.94 (m, 8H, piperazine), 4.20 (brs, 2H, piperazine), 4.38 (s, 2H, CO-CH_2), 4.50 (s, 1H, -OH), 6.68 (t, 1H, J = 4.7 Hz, Ar-H), 8.40 (d, 2H, J = 4.7 Hz, Ar-H). ^{13}C-NMR (125 MHz, DMSO-d$_6$, ppm) δ 31.15 (S-CH_2), 41.96, 43.51, 45.63, 50.27, 51.73, 53.02, 58.97 (CH_2), 59.97 (CH_2), 110.97 (pyrimidine C_5), 158.46 (pyrimidine C_4, C_6), 161.57 (pyrimidine C_2), 165.78 (C=O), 194.74 (C=S). For $C_{17}H_{26}N_6O_2S_2$ calculated: 49.73% C, 6.38% H, 20.47% N; found: 49.87% C, 6.45% H, 20.44% N. HRMS (*m/z*): $[M+H]^+$ calcd for $C_{17}H_{26}N_6O_2S_2$: 411.1631; found 411.1628.

2-[4-(Pyrimidin-2-yl)piperazin-1-yl]-2-oxoethyl 4-(2-(dimethylamino)ethyl)piperazine-1-carbodithioate (2d)

Yield 70%, m.p. 113–117 °C. IR ν_{max}(cm^{-1}): 3016 (aromatic C–H), 2908 (aliphatic C–H), 1633 (amide C=O), 1581–1423 (C=C and C=N), 1257–1029 (C–N and C–O). ^{1}H-NMR (500 MHz, DMSO-d$_6$, ppm) δ 2.30–2.33 (m, 10H, $(CH_2)_2$-N-$(CH_3)_2$), 2.51–2.60 (m, 4H,

piperazine), 3.32–4.82 (m, 8H, piperazine), 3.95 (brs, 2H, piperazine), 4.21 (brs, 2H, piperazine), 4.38 (s, 2H, CO-CH_2), 6.68 (t, 1H, $J = 4.7$ Hz, pyrimidine), 8.40 (d, 2H, $J = 4.7$ Hz, pyrimidine). ^{13}C-NMR (125 MHz, DMSO-d_6, ppm) δ 29.45 (S-CH_2), 41.96, 43.50, 45.08, 45.62, 50.20, 51.65, 54.33, 55.94, 110.97 (pyrimidine C_5), 158.46 (pyrimidine C_4, C_6), 161.56 (pyrimidine C_2), 165.77 (C=O), 194.80 (C=S). For $C_{19}H_{31}N_7OS_2$ calculated: 52.15% C, 7.14% H, 22.40% N; found: 52.08% C, 7.18% H, 22.45% N. HRMS (*m/z*): $[M + H]^+$ calcd for $C_{19}H_{31}N_7OS_2$: 438.2104; found 438.2094.

2-[4-(Pyrimidin-2-yl)piperazin-1-yl]-2-oxoethyl 4-cyclohexylpiperazine-1-carbodithioate (2e)

Yield 72%, m.p. 188–190 °C. IR ν_{max}(cm^{-1}): 3064 (aromatic C–H), 2924 (aliphatic C–H), 1647 (amide C=O), 1581–1419 (C=C and C=N, NO_2), 1278–1002 (C–N and C–O). ^{1}H-NMR (500 MHz, DMSO-d_6, ppm) δ 1.17–1.22 (m, 4H, cyclohexyl), 1.56–1.58 (m, 2H, cyclohexyl), 1.73–1.76 (m, 4H, cyclohexyl), 2.29 (brs, 1H, cyclohexyl), 2.58 (brs, 4H, piperazine), 3.55 (t, 2H, $J = 4.7$ Hz, piperazine), 3.66 (brs, 2H, piperazine), 3.71 (brs, 2H, piperazine), 3.82 (brs, 2H, piperazine), 3.92 (brs, 2H, piperazine), 4.19 (brs, 2H, piperazine), 4.37 (s, 2H, CO-CH_2), 6.68 (t, 1H, $J = 4.8$ Hz, pyrimidine), 8.40 (d, 2H, $J = 4.8$ Hz, pyrimidine). ^{13}C-NMR (125 MHz, DMSO-d_6, ppm) δ 25.68, 26.26, 28.77 (S-CH_2), 41.96, 43.51, 45.63, 48.61, 62.73, 110.97 (pyrimidine C_5), 158.46 (pyrimidine C_4, C_6), 161.57 (pyrimidine C_2), 165.80 (C=O), 194.53 (C=S). For $C_{21}H_{32}N_6OS_2$ calculated: 56.22% C, 7.19% H, 18.73% N; found: 56.28% C, 7.12% H, 18.78% N. HRMS (*m/z*): $[M + H]^+$ calcd for $C_{21}H_{32}N_6OS_2$: 449.2152; found 449.2144.

2-[4-(Pyrimidin-2-yl)piperazin-1-yl]-2-oxoethyl 4-phenylpiperazine-1-carbodithioate (2f)

Yield 67%, m.p. 186–188 °C. IR ν_{max}(cm^{-1}): 3070 (aromatic C–H), 2972 (aliphatic C–H), 1645 (amide C=O), 1581–1423 (C=C and C=N), 1273–1004 (C–N and C–O). ^{1}H-NMR (500 MHz, DMSO-d_6, ppm) δ 3.33–3.39 (m, 4H, piperazine), 3.77–3.79 (m, 4H, piperazine), 3.90–4.02 (m, 4H, piperazine), 4.26–4.29 (m, 2H, piperazine), 4.44 (s, 2H, CO-CH_2), 4.55 (brs, 2H, piperazine), 6.61 (t, 1H, $J = 4.8$ Hz, pyrimidine), 6.99–7.05 (m, 3H, phenyl), 7.34 (t, 2H, $J = 7.9$ Hz, phenyl), 8.39 (d, 2H, $J = 4.8$ Hz, pyrimidine). ^{13}C-NMR (125 MHz, DMSO-d_6, ppm) δ 30.76 (S-CH_2), 40.36, 42.16, 43.70, 45.94, 49.38, 110.43 (pyrimidine C_5), 116.91, 129.50, 157.68 (pyrimidine C_4, C_6), 161.28 (pyrimidine C_2), 166.04 (C=O), 195.76 (C=S). For $C_{21}H_{26}N_6OS_2$ calculated: 56.99% C, 5.92% H, 18.99% N; found: 56.91% C, 5.94% H, 18.82% N. HRMS (*m/z*): $[M + H]^+$ calcd for $C_{21}H_{26}N_6OS_2$: 443.1682; found 443.1682.

2-[4-(Pyrimidin-2-yl)piperazin-1-yl]-2-oxoethyl 4-(p-tolyl)piperazine-1-carbodithioate (2 g)

Yield 62%, m.p. 157–160 °C. IR ν_{max}(cm^{-1}): 3034 (aromatic C–H), 2980 (aliphatic C–H), 1647 (amide C=O), 1577–1417 (C=C and C=N), 1301–1033 (C–N and C–O). ^{1}H-NMR (500 MHz, $CDCl_3$, ppm) δ 2.62 (s, 3H, CH_3), 3.09–3.46 (m, 8H, piperazine), 3.73–3.91 (m, 8H, piperazine), 4.45 (brs, 2H, CO-CH_2), 6.51 and 6.56 (dt, 1H, $J_1 = 25.2$ Hz, $J_2 = 4.8$ Hz, pyrimidine), 6.85–6.92 (m, 4H, phenyl), 8.33 and 8.35 (dd, 2H, $J_1 = 12.8$ Hz, $J_2 = 4.7$, pyrimidine). ^{13}C-NMR (125 MHz, DMSO-d_6, ppm) δ 29.70 (S-CH_2), 41.76, 43.66, 45.53, 46.97, 49.17, 50.80, 53.01, 55.54, 61.54, 110.00, 110.47, 114.51, 114.61, 118.71, 118.93, 119.00, 119.45, 144.64, 145.56, 154.23, 154.94, 157.71, 157.79 (pyrimidine C_4, C_6), 161.62 (pyrimidine C_2), 163.74, 168.12 (C=O), 194.52 (C=S). For $C_{22}H_{28}N_6OS_2$ calculated: 57.87% C, 6.18% H, 18.40% N; found: 57.94% C, 6.24% H, 18.50% N. HRMS (*m/z*): $[M + H]^+$ calcd for $C_{22}H_{28}N_6OS_2$: 456.64; found 457.10.

2-[4-(Pyrimidin-2-yl)piperazin-1-yl]-2-oxoethyl 4-(4-chlorophenyl)piperazine-1-carbodithioate (2 h)

Yield 66%, m.p. 190–192 °C. IR ν_{max}(cm^{-1}): 3059 (aromatic C–H), 2989 (aliphatic C–H), 1653 (amide C=O), 1581–1429 (C=C and C=N), 1269–1029 (C–N and C–O). ^{1}H-NMR (500 MHz, DMSO-d_6, ppm) δ 3.25–3.30 (m, 4H, piperazine), 3.55–3.84 (8H, piperazine), 4.11 (brs, 2H, piperazine), 4.35 (brs, 2H, piperazine), 4.41 (s, 2H, CO-CH_2), 6.66 (m, 1H, pyrimidine), 6.93–6.97 (m, 2H, phenyl), 7.22 (d, 1H, $J = 9.0$ Hz, phenyl), 7.27 (d, 1H, $J = 9.0$ Hz, phenyl), 8.38–8.40 (m, 2H, pyrimidine). ^{13}C-NMR (125 MHz, DMSO-d_6, ppm) δ 30.51 (S-CH_2), 41.49 41.96, 43.51, 44.26, 47.74, 48.56, 52.76, 60.95, 110.91, 110.97, 117.25, 117.32, 122.79, 123.17, 129.05, 129.21, 149.29, 150.28, 158.44, 158.46 (pyrimidine C_4, C_6), 161.57, 161.66, 165.72, 168.03 (C=O), 195.16 (C=S). For $C_{21}H_{25}ClN_6OS_2$ calculated: 52.87% C, 5.28% H, 17.62% N; found: 57.96% C, 5.34% H, 17.54% N. HRMS (*m/z*): $[M + H]^+$ calcd for $C_{21}H_{25}ClN_6OS_2$: 477.06; found 477.21.

2-[4-(Pyrimidin-2-yl)piperazin-1-yl]-2-oxoethyl 4-(4-fluorophenyl)piperazine-1-carbodithioate (2i)

Yield 73%, m.p. 191–193 °C. IR ν_{max}(cm^{-1}): 3076 (aromatic C–H), 2968 (aliphatic C–H), 1639 (amide C=O), 1579–1436 (C=C and C=N), 1271–1028 (C–N and C–O). ^{1}H-NMR (500 MHz, DMSO-d_6, ppm) δ 3.21 (brs, 4H, piperazine), 3.26–3.31 (m, 2H, piperazine), 3.55–3.82 (m, 6H, piperazine), 4.10 (brs, 2H, piperazine), 4.35 (brs, 2H, piperazine), 4.38 (s, 2H, CO-CH_2), 6.67 (t, 1H, $J = 4.8$ Hz, pyrimidine), 6.96–6.98 (m, 2H, phenyl), 7.05–7.09 (m, 2H, phenyl), 8.38 (d, 2H, $J = 4.8$ Hz, pyrimidine). ^{13}C-NMR (125 MHz, DMSO-d_6, ppm) δ 30.48 (S-CH_2), 42.01, 43.49, 45.61, 48.99, 111.05 (pyrimidine C_5), 115.81, 115.98, 117.95, 118.01, 147.38, 147.39, 155.85, 157.73, 158.48, 161.50 (pyrimidine C_2), 165.91 (C=O), 195.18 (C=S). For $C_{21}H_{25}FN_6OS_2$ calculated: 54.76% C, 5.47% H, 18.25% N; found: 54.82% C, 5.65% H, 18.34% N. HRMS (*m/z*): $[M + H]^+$ calcd for $C_{21}H_{25}FN_6OS_2$: 461.1588; found 461.1584.

2-[4-(Pyrimidin-2-yl)piperazin-1-yl]-2-oxoethyl 4-(4-nitrophenyl)piperazine-1-carbodithioate (2j)

Yield 64%, m.p. 243–247 °C. IR ν_{max}(cm^{-1}): 3026 (aromatic C–H), 2953 (aliphatic C–H), 1654 (amide C=O), 1595–1417 (C=C and C=N), 1579 and 1303 (NO_2), 1288–1001 (C–N and C–O). ^{1}H-NMR (500 MHz, $CDCl_3$, ppm) δ 3.62–3.66 (m, 4H, piperazine), 3.76–3.83 (m, 4H, piperazine), 4.02 (brs, 2H, piperazine), 4.18 (brs, 2H, piperazine), 4.30–4.49 (s, 6H, CO-CH_2 and piperazine), 6.76 (s, 1H, pyrimidine), 6.83 (d, 2H, $J = 9.4$ Hz, phenyl), 8.19 (d, 2H, $J = 9.3$ Hz, phenyl), 8.50 (d, 2H, $J = 4.9$ Hz, pyrimidine). ^{13}C-NMR (125 MHz, DMSO-d_6, ppm) δ 29.70 (S-CH_2), 39.99, 41.99, 44.39, 44.95, 45.63, 45.75, 51.36, 110.11 (pyrimidine C_5), 112.30, 112.70, 125.97, 126.06, 139.13, 153.62, 157.84 (pyrimidine C_4, C_6), 161.39 (pyrimidine C_2), 165.98 (C=O), 195.95 (C=S). For $C_{21}H_{25}N_7O_3S_2$ calculated: 51.73% C, 5.17% H, 20.11% N; found: 51.84% C, 5.25% H, 20.18% N. HRMS (*m/z*): $[M + H]^+$ calcd for $C_{21}H_{25}N_7O_3S_2$: 488.1533; found 488.1528.

2[(4-(Pyrimidin-2-yl)piperazin-1-yl]-2-oxoethyl 4-benzylpiperazine-1-carbodithioate (2k)

Yield 69%, m.p. 145–150 °C. IR ν_{max}(cm^{-1}): 3013 (aromatic C–H), 2931 (aliphatic C–H), 1635 (amide C=O), 1581–1415 (C=C and C=N), 1251–1024 (C–N and C–O). ^{1}H-NMR (500 MHz, DMSO-d_6, ppm) δ 2.62 (brs, 4H, piperazine), 3.62–4.06 (m, 12H, piperazine) 4.20 (brs, 2H, CH_2), 4.38 (s, 2H, CO-CH_2), 6.57 (t, 1H, $J = 4.8$ Hz, pyrimidine), 7.29–7.37 (m, 5H, phenyl), 8.35 (d, 2H, $J = 6.8$ Hz,

pyrimidine). ^{13}C-NMR (125 MHz, DMSO-d_6, ppm) δ 13.80, 29.70 (S-CH_2), 39.25, 40.35, 42.20, 43.46, 46.02, 49.74, 51.32, 52.20, 62.34, 70.71, 110.52, 110.62 (pyrimidine C_5), 127.73, 128.53, 129.33, 157.80 (pyrimidine C_4, C_6), 161.51 (pyrimidine C_2), 165.44 (C=O), 195.31 (C=S). For $C_{22}H_{28}N_6OS_2$ calculated: 57.87% C, 6.18% H, 18.40% N; found: 57.69% C, 6.26% H, 18.48% N. HRMS (*m/z*): $[M+H]^+$ calcd for $C_{22}H_{28}N_6OS_2$: 457.1839; found 457.1833.

2-[4-(Pyrimidin-2-yl)piperazin-1-yl]-2-oxoethyl 4-(4-methylbenzyl)piperazine-1-carbodithioate (2 l)

Yield 72%, m.p. 144–146 °C. IR ν_{max}(cm^{-1}): 3022 (aromatic C–H), 2927 (aliphatic C–H), 1635 (amide C=O), 1579–1411 (C=C and C=N), 1257–1020 (C–N and C–O). ^{1}H-NMR (500 MHz, DMSO-d_6, ppm) δ 2.37 (s, 3H, CH_3), 2.72 (brs, 4H, piperazine), 3.72–3.75 (m, 6H, piperazine), 3.85–4.17 (m, 6H, piperazine), 4.18 (s, 2H, C-CH_2), 4.37 (s, 2H, CO-CH_2), 6.60 (t, 1H, $J=4.7$, pyrimidine), 7.20 (d, 2H, $J=7.7$ Hz, phenyl), 7.29 (d, 2H, $J=7.7$ Hz, phenyl), 8.35 (d, 2H, $J=4.8$ Hz, pyrimidine). ^{13}C-NMR (125 MHz, DMSO-d_6, ppm) δ 21.16, 29.30 (S-CH_2), 40.50, 42.22, 43.46, 46.02, 51.76, 61.77, 110.55 (pyrimidine C_5), 129.43, 157.80 (pyrimidine C_4, C_6), 161.51 (pyrimidine C_2), 165.96 (C=O), 194.80 (C=S). For $C_{23}H_{30}N_6OS_2$ calculated: 58.70% C, 6.43% H, 17.87% N; found: 58.62% C, 6.29% H, 17.82% N. HRMS (*m/z*): $[M+H]^+$ calcd for $C_{23}H_{30}N_6OS_2$: 471.1995; found 471.1976.

2-[4-(Pyrimidin-2-yl)piperazin-1-yl]-2-oxoethyl 4-benzhydrylpiperazine-1-carbodithioate (2m)

Yield 70%, m.p. 187–188 °C. IR ν_{max}(cm^{-1}): 3080 (aromatic C–H), 2926 (aliphatic C–H), 1647 (amide C=O), 1581–1435 (C=C and C=N), 1259–1028 (C–N and C–O). ^{1}H-NMR (500 MHz, DMSO-d_6, ppm) δ 2.77 (brs, 4H, piperazine), 3.74–3.97 (m, 8H, piperazine), 4.39 (brs, 7H, CO-CH_2, CH, piperazine), 6.58 (t, 1H, $J=4.7$ Hz, pyrimidine), 7.26–7.87 (m, 10H, phenyl), 8.36 (d, 2H, $J=8$ Hz, pyrimidine). ^{13}C-NMR (125 MHz, DMSO-d_6, ppm) δ 29.49 (S-CH_2), 40.49, 42.25, 43.48, 45.98, 51.68, 110.57 (pyrimidine C_5), 128.29, 129.50, 157.27 (pyrimidine C_4, C_6), 161.43 (pyrimidine C_2), 165.23 (C=O), 194.74 (C=S). For $C_{28}H_{32}N_6OS_2$ calculated: 63.13% C, 6.05% H, 15.78% N; found: 63.18% C, 6.11% H, 15.84% N. HRMS (*m/z*): $[M+H]^+$ calcd for $C_{28}H_{32}N_6OS_2$: 533.2152; found 533.2144.

2-[4-(Pyrimidin-2-yl)piperazin-1-yl]-2-oxoethyl 4-(pyrimidin-2-yl)piperazine-1-carbodithioate (2n)

Yield 68%, m.p. 250–254 °C. IR ν_{max}(cm^{-1}): 3070 (aromatic C–H), 2908 (aliphatic C–H), 1633 (amide C=O), 1583–1421 (C=C and C=N), 1259–1029 (C–N and C–O). ^{1}H-NMR (500 MHz, DMSO-d_6, ppm) δ 3.70–3.87 (m, 10H, piperazine), 4.09 (brs, 4H, piperazine), 4.31 (brs, 2H, piperazine), 4.40 (s, 2H, CO-CH_2), 6.67–6.71 (m, 2H, Ar-H), 8.38–8.41 (m, 4H, Ar-H). ^{13}C-NMR (125 MHz, DMSO-d_6, ppm) δ 31.13 (S-CH_2), 42.96, 44.35, 44.90, 45.69, 45.70, 51.34, 110.53 (pyrimidine C_5), 158.49 (pyrimidine C_4, C_6), 161.46 (pyrimidine C_2), 165.85 (C=O), 194.50 (C=S). For $C_{19}H_{24}N_8OS_2$ calculated: 51.33% C, 5.44% H, 25.21% N; found: 51.43% C, 5.57% H, 25.29% N. HRMS (*m/z*): $[M+H]^+$ calcd for $C_{19}H_{24}N_8OS_2$: 444.58; found 445.60.

MAO activity assay

Enzyme activity assay was performed according to the modified fluorimetric method reported by Matsumoto et al.[31] The entire materials used in enzymatic assay were purchased from Sigma-Aldrich Chemicals (St. Louis, MO). All of the pipettings in the assay were performed by Biotek Precision robotic system (BioTek Instruments Inc., Winooski, VT). The assay was performed in 96-well black plates to prevent light effect on MAO enzymes. Phosphate buffer (0.1 M, pH =7.4) was used for preparation of stock solutions (5 mg/mL) of both human recombinant MAO-A and MAO-B enzymes. Enzyme stock solutions were further diluted with assay buffer to get a final concentration 0.006 mg/mL for MAO-A and 0.015 mg/mL for MAO-B. Kynuramine was dissolved in sterilized distilled water to get stock solution (25 mM) and then diluted with assay buffer to get a final concentration of 40 μM for MAO-A enzyme and 20 μM for MAO-B enzyme. Synthesized compounds and reference drugs (moclobemide for MAO-A enzyme and selegiline for MAO-B enzyme) were dissolved in 2% DMSO to dilute to 10^{-3} M and 10^{-4} M concentrations (100 μL/well). Then either MAO-A or MAO-B enzyme solutions were added (50 μL/well). After 10-min incubation at 37 °C, kynuramine (50 μL/well) was added and enzyme–substrate reaction was initiated. The plate was incubated for 20 min at 37 °C and then reaction was ended by using of 2 N NaOH (75 μL/well). The fluorimetric read from top at 310/380 nm excitation/emission wavelength pair was performed by BioTek-Synergy H1 multimode microplate reader (BioTek Instruments Inc., Winooski, VT). The same procedure was followed for further concentrations (10^{-5} to 10^{-9} M, 100 μL/well) of reference drugs and selected compounds, showing ≥50% inhibition at initial concentrations (10^{-3} and 10^{-4} M, 100 μL/well). The IC_{50} value was calculated from the plots of enzyme activity against concentrations by applying regression analyses on GraphPad Prism Version 5.

Enzyme kinetics

The MAO-A enzyme kinetic of the most active compound **2j** was studied. The nature of MAO-A inhibition, caused by this compound, was investigated by the graphical analysis of steady-state inhibition data. Lineweaver–Burk plots identified the compound **2j** as a mix-typed inhibitor, due to the different intercepts on both the y- and x-axes (Figure 2). The values of K_m and V_{max} were calculated by nonlinear regression according to literature[31] and found as 48.37 and 5.34, respectively.

Molecular properties and drug-likeness score

Molecular properties identify some physicochemical parameters of a molecule which help to evaluate whether a compound could be a potential therapeutic agent. Also, oral bioavailability of a molecule is known to play an important role for the development of bioactive derivatives[32]. Therefore, some physicochemical properties and drug-likeness score of the synthesized compounds were calculated using Molinspiration[33] and MolSoft[34] softwares and the obtained data were represented in Table 1. The computational study for prediction of ADME properties of the molecules was performed by determination of log P, topological polar surface area (TPSA), molecular weight (MW), number of hydrogen donors (nON) and acceptors (nOHNH), number of rotable bonds (nrotb) and volume. The absorption percentage (% ABS) of the compounds were also calculated using the formula % Absorption = 109 − (0.345 × TPSA) placing the predicted TPSA values[35]. Calculated % ABS of the compounds (**2a-n**) were found between the range of 73.94–89.75%. Good intestinal absorption, reduced molecular flexibility (measured by the number of rotatable bonds), low polar surface area or total hydrogen bond count (sum of donors and acceptors) are important molecular descriptors for high oral

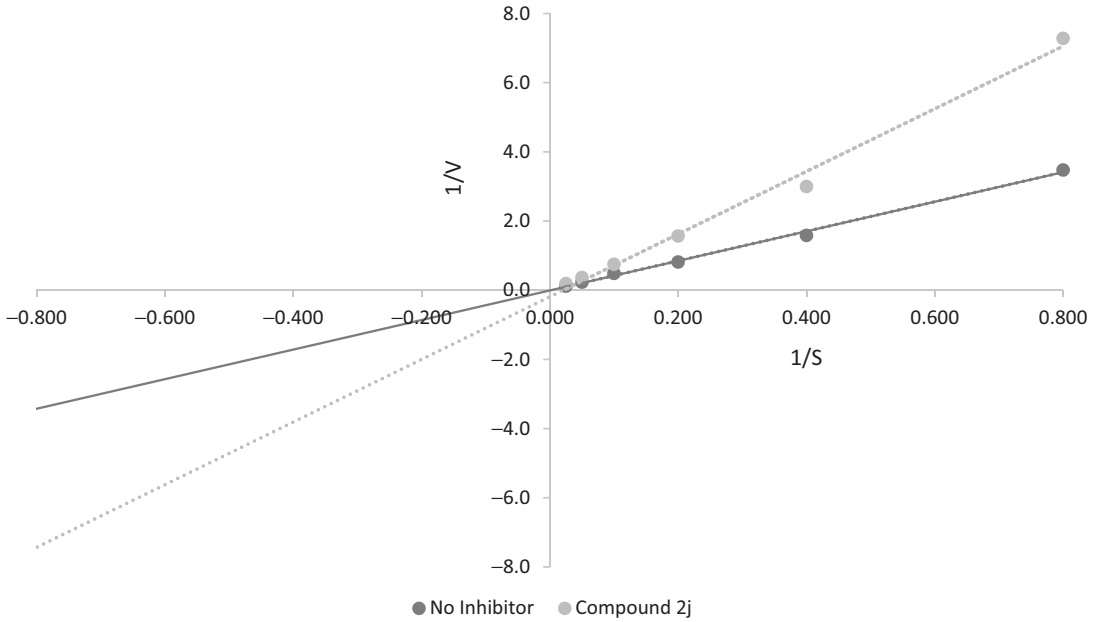

Figure 2. Lineweaver–Burk plots for compound **2j** (IC_{50} = 23.10 μM). Substrate (kynuramine) concentrations used: 40, 20, 10, 5, 2.5 and 1.25 μM. 1/V: 1/velocity of reaction [1/(nmoles/min/mg protein)], 1/S: 1/substrate concentration (1/μM).

Table 1. *In silico* physicochemical parameters of the compounds **2a-n**.

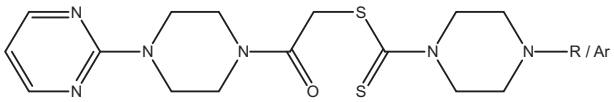

2a-n

Comp	R/Ar	% ABS	Log P	TPSA	MW	nON	nOHNH	nrotb	Volume	DLS*
2a	$-CH_3$	89.75	0.82	55.81	380.54	7	0	5	337.93	0.72
2b	$-C_2H_5$	89.75	1.20	55.81	394.57	7	0	6	354.74	0.70
2c	$-C_2H_5OH$	82.77	0.19	76.03	410.57	8	1	7	362.99	0.92
2d	$-C_2H_5N(CH_3)_2$	88.63	0.85	59.05	437.64	8	0	8	400.88	1.52
2e	−cyclohexyl	89.75	2.73	55.81	448.66	7	0	6	411.37	0.33
2f	−phenyl	89.75	2.52	55.81	442.61	7	0	6	392.78	0.0
2g	4-CH_3 phenyl	89.75	2.96	55.81	456.64	7	0	6	409.34	−0.03
2h	4-Cl phenyl	89.75	3.19	55.81	477.06	7	0	6	406.32	0.38
2i	4-F phenyl	89.75	2.68	55.81	460.60	7	0	6	397.71	0.17
2j	4-NO_2 phenyl	73.94	2.48	101.63	487.61	10	0	7	416.12	−0.30
2k	benzyl	89.75	2.22	55.81	456.64	7	0	7	409.58	0.83
2l	4-CH_3 benzyl	89.75	2.96	55.81	470.64	7	0	6	409.34	0.87
2m	−diphenyl methyl	89.75	4.00	55.81	532.74	7	0	8	481.02	1.56
2n	−2-pyrimidinyl	80.85	1.23	81.59	444.59	9	0	6	384.47	−0.22
St. 1	–	107.88	2.64	3.24	187.29	1	0	4	202.64	1.03
St. 2	–	108.42	1.69	41.57	268.74	4	1	4	240.70	1.36

% ABS: Percentage of absorption was calculated using the formula 109 − (0.345 × TPSA).
Log P: log octanol/water partition coefficient; MW: molecular weight; TPSA: total polar surface area; nON: no. of hydrogen acceptors; nOHNH: no. of hydrogen donors; nrotb: no. of rotatable bonds were calculated using Molinspiration Calculation of Molecular Properties toolkit.
*DLS: Drug-likeness Model Score was calculated using MolSoft 2016 Drug-Likeness and molecular property prediction toolkit.
Standard 1: Selegiline; Standard 2: Moclobemide.

bioavailability[36]. Considering Lipinski's rule of five[37], all synthesized compounds have hydrogen bond donors and log P values smaller than five, hydrogen bond acceptors smaller than 10 and polar surface area smaller than 140. Besides, molecular weights of the compounds are in accordance with the value smaller than 500 dalton except compound **2m**. According to the stated data, all compounds are in the specified values to be a potential drug with good physicochemical properties such as solubility, lipophilicity, flexibility and membrane permeability.

Drug-likeness score is also assigned for all compounds and standard drugs according to MolSoft's chemical fingerprints mode consisted of 5K of marketed drugs from World Drug Index (positives) and 10K of carefully selected non-drug compounds (negatives). The values were found between −0.30 and 1.56 for synthesized compounds (**2a-n**) and 1.03–1.36 for standard drugs. According to all these data, two active compounds **2j** bearing 4-nitrophenyl moiety and **2m** bearing diphenylmethyl moiety did not correlate these informations. Compound **2j** is in accordance with Lipinski's rule of five, but the predicted drug-likeness score of it is the lowest one, −0.30 among the others. Compound **2m** possesses the highest drug-likeness score (1.56) which is also higher than standard drugs, although molecular weight of the compound

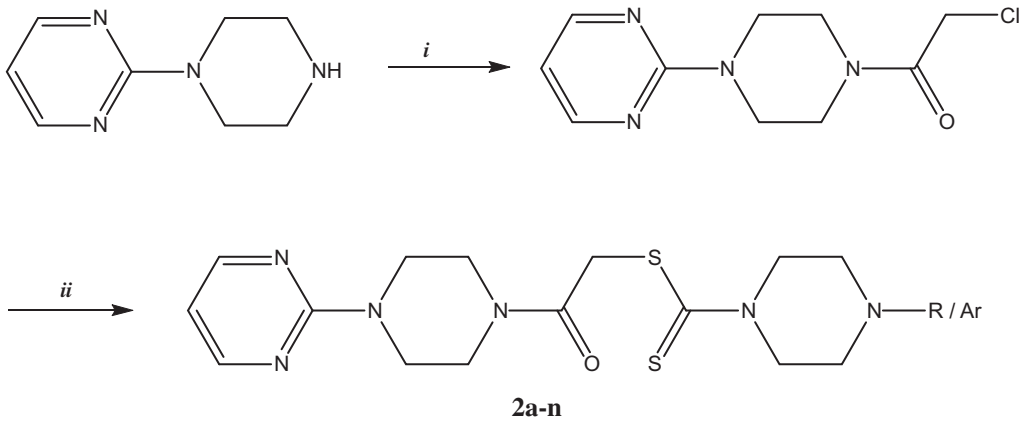

Figure 3. Synthesis of the compounds **2a-n**. Reactants, reagents and conditions: *i:* $ClCOCH_2Cl$, Et_3N, THF, 0–5 °C, 3 h; *ii*: Potassium/Sodium salts of substituted piperazine dithiocarbamates, K_2CO_3, acetone, r.t, 5 h.

(MW = 532) exceeds Lipinski's limit. However, compound **2m** possesses the highest log P (4.00) due to bearing two aromatic rings that provides lipophilic character which is suitable to cross BBB (blood brain barrier)[38].

Molecular docking

Docking studies were applied to discover and designate the assumed binding modes in MAO-A enzyme active site of the most potent compound **2j** in the compound series and protein–ligand interactions analysis was performed using human MAO-A X-ray crystal structure complex with 7-methoxy-1-methyl-9H-β-carboline (harmine), retrieved from Protein Data Bank server (PDB ID: 2Z5X) (www.pdb.org). Docking calculations were performed with the program AutoDock Vina[39]. AutoDock Tools (ADT, Version 1.5.6)[40] were used to add polar hydrogen atoms and partial charges for protein and ligand, which were saved in pdbqt format. For docking studies initial protein was prepared. In the PDB crystallographic structure any co-crystallized solvent and the ligand were removed. Docking procedure was carried out following the same protocol described previously[41]. The grid center coordinates were x = 41.126, y = 26.795, z = −15.023 and the size coordinates were x = 60, y = 60, z = 60 with a spacing of 0.375 Å. AutoDock Vina was used to dock the ligand into the active site of the protein. The poses of the docked ligand were analyzed and the results were visualized by PyMOL 1.6.X[42].

Results and discussion

Chemistry

A new series of 2-[4-(pyrimidin-2-yl)piperazin-1-yl]-2-oxoethyl 4-substituted piperazine-1-carbodithioate derivatives (**2a-n**) were synthesized in this study (Figure 3). Primarily, dithiocarbamate potassium salt of some secondary amines and 2-chloro-*N*-[4-(2-pyrimidinyl)piperazine]acetamide were gained according to well-known synthetic procedures as previously reported[43]. The structures of the final compounds were elucidated by using spectroscopic techniques. In the IR spectra of the compounds (**2a-n**), characteristic amide carbonyl functions were observed at 1633–1663 cm^{-1} region. The other specific bands were observed at 1581–1417 cm^{-1} and 1301–1002 cm^{-1} belong to C=C, C=N and C−N, C−O bonds. The ^1H NMR spectra of all final compounds exhibited singlet peaks resulting from resonances of the acetamide residue assigned to -S-CH_2-protons at 4.30–4.49 ppm. The protons of pyrimidine ring were resonated as doublet peaks at 8.35–8.41 ppm and as triplet peaks at 6.51–6.68 ppm. The other carbon atoms in aromatic region were observed at the range of 6.83–7.87 ppm, consistently. The signals correspond to piperazine ring were observed at about 2.36–4.35 ppm, a broad field as triplet or broad singlet peaks. In the ^{13}C NMR spectrum of the compounds, the signals belong to C=S and C=O carbons were determined at 194.29–195.95 ppm and 165.15–168.12 ppm, as estimated. The carbon atoms belong to C-S group and piperazine ring were resonated at 28.77–31.15 ppm and 41.95–61.77 ppm, respectively. In the mass spectra of the compounds, M + 1 peaks agreed well with the calculated molecular weight of the target compounds. Elemental analysis results were also found within 0.4% of the theoretical values.

Monoamine oxidase inhibitory activity

The synthesized compounds (**2a-n**) were investigated for their MAO-A and MAO-B inhibitory activity by an *in vitro* fluorimetric method. The fundamental of the activity determination is based on the ability of both MAO-A and MAO-B enzymes to metabolize non-fluorescent kynuramine, which is a suitable substrate for both isozymes, to the fluorescent product 4-hydroxyquinoline. MAO-inhibitory effect of the test compounds was correlated to the amount of 4-hydroxyquinoline formed. DMSO was considered as control (100% activity). In the assay as reference drug, moclobemide and selegiline were used. The inhibitory activity results are shown in Tables 2 and 3.

In general, when the results were analyzed, it was observed that the synthesized compounds are more potent against MAO-A enzyme as regards MAO-B enzyme. The compounds **2i**, **2j** and **2m** displayed over 50% inhibition against MAO-A enzyme at 10^{-3} M concentration. The compounds **2f**, **2j**, **2l** and **2m** exhibited significant inhibition profile against MAO-B enzyme at 10^{-3} M concentration. When the percentage inhibition rates at 10^{-4} M concentration were compared, the compounds **2j** and **2m** showed over 50% inhibition against MAO-A enzyme. So it is understood that these derivatives are selective MAO-A enzyme inhibitors.

Due to their inhibition potency (>50%) at 10^{-3} and 10^{-4} M, the compounds **2j** and **2m** were studied in more concentrations (10^{-5} M to 10^{-9} M) so as to calculate IC_{50} values (Figure 4). According to enzyme inhibition profiles, compound **2j** is the most active derivative owing to its MAO-A inhibiton with an IC_{50} value of 23.10 μM.

Table 2. Inhibitory activity (%) of the compounds against MAO-A enzyme.

	MAO-A inhibition %							
Comp.	10^{-3} M	10^{-4} M	10^{-5} M	10^{-6} M	10^{-7} M	10^{-8} M	10^{-9} M	MAO-A IC_{50} (μM)
2a	12.84 ± 0.59	7.33 ± 0.19	n.d	n.d	n.d	n.d	n.d	>1000
2b	11.52 ± 0.38	6.86 ± 0.21	n.d	n.d	n.d	n.d	n.d	>1000
2c	15.88 ± 0.55	9.27 ± 0.27	n.d	n.d	n.d	n.d	n.d	>1000
2d	18.74 ± 0.52	7.39 ± 0.30	n.d	n.d	n.d	n.d	n.d	>1000
2e	16.75 ± 0.42	5.90 ± 0.15	n.d	n.d	n.d	n.d	n.d	>1000
2f	33.33 ± 1.30	31.25 ± 0.88	n.d	n.d	n.d	n.d	n.d	>1000
2g	37.50 ± 1.42	33.33 ± 0.99	n.d	n.d	n.d	n.d	n.d	>1000
2h	13.45 ± 0.38	6.70 ± 0.22	n.d	n.d	n.d	n.d	n.d	>1000
2i	58.33 ± 1.75	39.58 ± 0.95	n.d	n.d	n.d	n.d	n.d	>100
2j	91.66 ± 2.74	69.83 ± 1.85	42.45 ± 1.18	29.70 ± 0.72	20.19 ± 0.64	16.05 ± 0.40	11.53 ± 0.29	23.10
2k	19.81 ± 0.59	6.15 ± 0.18	n.d	n.d	n.d	n.d	n.d	>1000
2l	32.31 ± 0.86	15.38 ± 0.61	n.d	n.d	n.d	n.d	n.d	>1000
2m	72.21 ± 2.05	60.46 ± 1.65	33.65 ± 0.93	28.16 ± 0.87	21.88 ± 0.74	15.77 ± 0.68	10.62 ± 0.41	24.14
2n	31.25 ± 0.94	25.00 ± 0.62	n.d	n.d	n.d	n.d	n.d	>1000
Moclobemide	94.12 ± 2.76	82.14 ± 2.69	60.45 ± 2.55	36.15 ± 1.98	22.13 ± 1.33	18.16 ± 0.81	14.12 ± 0.72	6.06

n.d: not determined.

Table 3. Inhibitory activity (%) of the compounds against MAO-B enzyme.

	MAO B inhibition %							
Comp.	10^{-3} M	10^{-4} M	10^{-5} M	10^{-6} M	10^{-7} M	10^{-8} M	10^{-9} M	MAO B IC_{50} (μM)
2a	10.23 ± 0.31	5.37 ± 0.22	n.d	n.d	n.d	n.d	n.d	>1000
2b	10.08 ± 0.42	5.65 ± 0.14	n.d	n.d	n.d	n.d	n.d	>1000
2c	12.30 ± 0.48	7.39 ± 0.25	n.d	n.d	n.d	n.d	n.d	>1000
2d	14.37 ± 0.58	8.40 ± 0.23	n.d	n.d	n.d	n.d	n.d	>1000
2e	12.60 ± 0.45	5.22 ± 0.18	n.d	n.d	n.d	n.d	n.d	>1000
2f	50.82 ± 1.02	31.15 ± 0.67	n.d	n.d	n.d	n.d	n.d	>100
2g	18.20 ± 0.82	10.76 ± 0.33	n.d	n.d	n.d	n.d	n.d	>1000
2h	40.98 ± 1.20	31.15 ± 1.07	n.d	n.d	n.d	n.d	n.d	>1000
2i	44.26 ± 1.13	27.86 ± 0.66	n.d	n.d	n.d	n.d	n.d	>1000
2j	53.01 ± 1.12	40.98 ± 0.94	n.d	n.d	n.d	n.d	n.d	>100
2k	13.08 ± 0.56	5.87 ± 0.22	n.d	n.d	n.d	n.d	n.d	>1000
2l	50.00 ± 1.37	15.00 ± 0.68	n.d	n.d	n.d	n.d	n.d	1000
2m	73.33 ± 1.52	40.00 ± 0.99	n.d	n.d	n.d	n.d	n.d	>100
2n	29.51 ± 0.74	22.95 ± 0.69	n.d	n.d	n.d	n.d	n.d	>1000
Selegiline	98.94 ± 2.06	94.73 ± 1.97	86.96 ± 1.82	79.22 ± 1.71	65.36 ± 1.12	43.27 ± 1.02	14.70 ± 0.25	0.038

n.d: not determined (no inhibition).

Enzyme kinetic studies

The same materials were used in MAO enzyme kinetic assay. The compound **2e** was prepared at IC_{50} concentration and then added to the wells (100 μL/well). Stock solution (25 mM) of kynuramine was diluted to final concentrations of 40, 20, 10, 5, 2.5 and 1.25 μM and then added to the wells (50 μL/well). After MAO-A enzyme was added to the plate (50 μL/well), incubation period at 37 °C for 20 min was started. The plate was read at 310/340 nm excitation/emission wavelength pair[31]. Control measurement without inhibitor was also determined simultaneously. The results were analyzed in Lineweaver–Burk plots using Microsoft Office Excel 2013.

Predictions of in silico *physicochemical parameters*

The physicochemical properties and drug-likeness score of the synthesized compounds were calculated using Molinspiration-Calculation of Molecular Properties and Bioactivity Score toolkit[33] and MolSoft-Drug-Likeness and molecular property prediction toolkit[34].

Molecular docking

Compound **2j** was docked into the active site of MAO-A using the program AutoDock Vina[39] in order to structurally understand the interactions with this target together with the inhibitor profile. Due to inhibition, data were determined on human MAOs, docking studies were run on the human model of the MAO-A. The 3D structure for human MAO-A retrieved from the Protein Data Bank server (PDB ID: 2Z5X) (www.rcsb.org)[41]. The best docking pose, showing residues in the active site, is seen in Figure 5. The docking study suggested that the compound **2j** is very compatible with the active site. The active region is consisting of these amino acids: Ile180, Asn181, Phe208, Gln215, Leu337 and Phe352. The carbonyl group in the structure settles down hydrogen bond with the amino group of Gln215. The nitrogen atom of piperazine moiety, near the pyrimidine, creates formation cation–π interaction with Phe208, whereas the other piperazine moiety does the same interaction with Leu337. The oxygen atoms of the nitro group are very significant in terms of polar interactions. The docking poses reveals that the nitro substituent interacts with Ile180 and Phe352 by formation of hydrogen bond. Also, it is thought that van der Waals interactions, between the compound **2j** and the active region of the enzyme, provide more steady binding.

Conclusion

Novel 2-[4-(pyrimidin-2-yl)piperazin-1-yl]-2-oxoethyl 4-substituted piperazine-1-carbodithioate derivatives (**2a-n**) were synthesized using (pyrimidin-2-yl)piperazin as starting material. The synthesized compounds were screened for their MAO-A and MAO-B enzyme

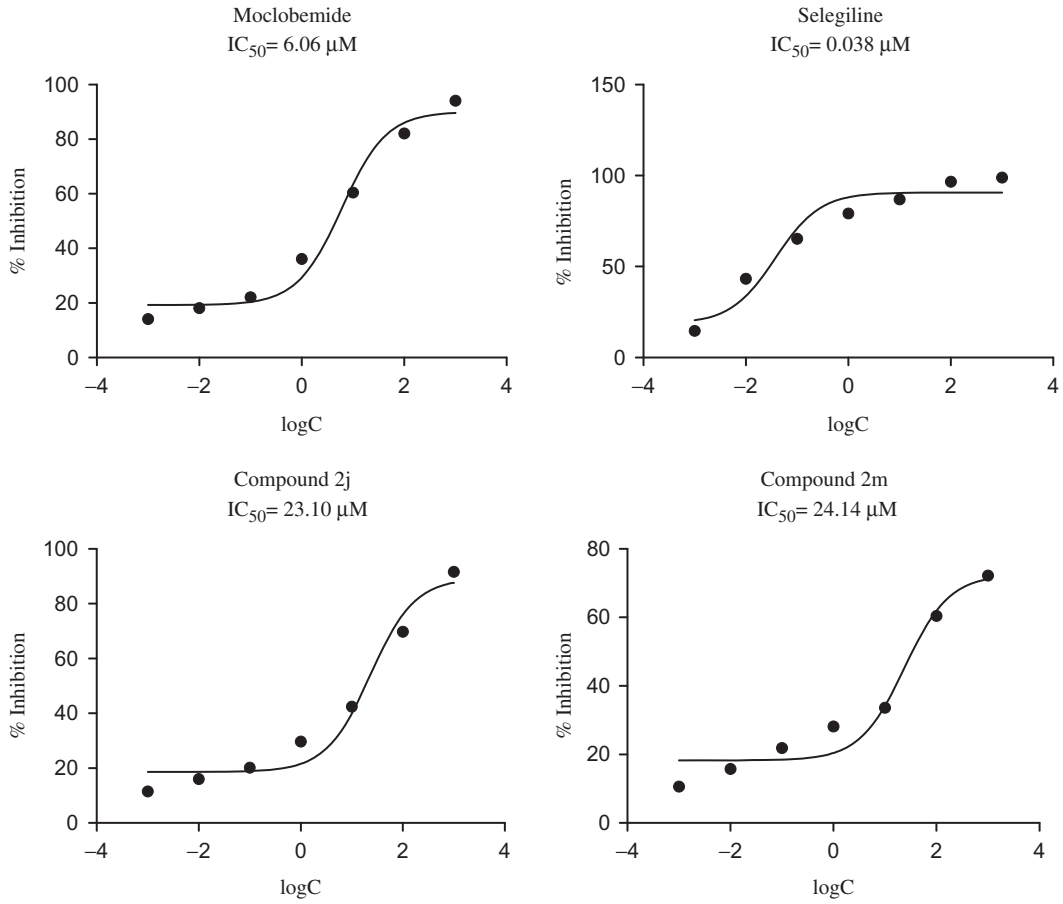

Figure 4. IC_{50} (µM) of the selected compounds and control drug against MAO-A and MAO-B enzymes.

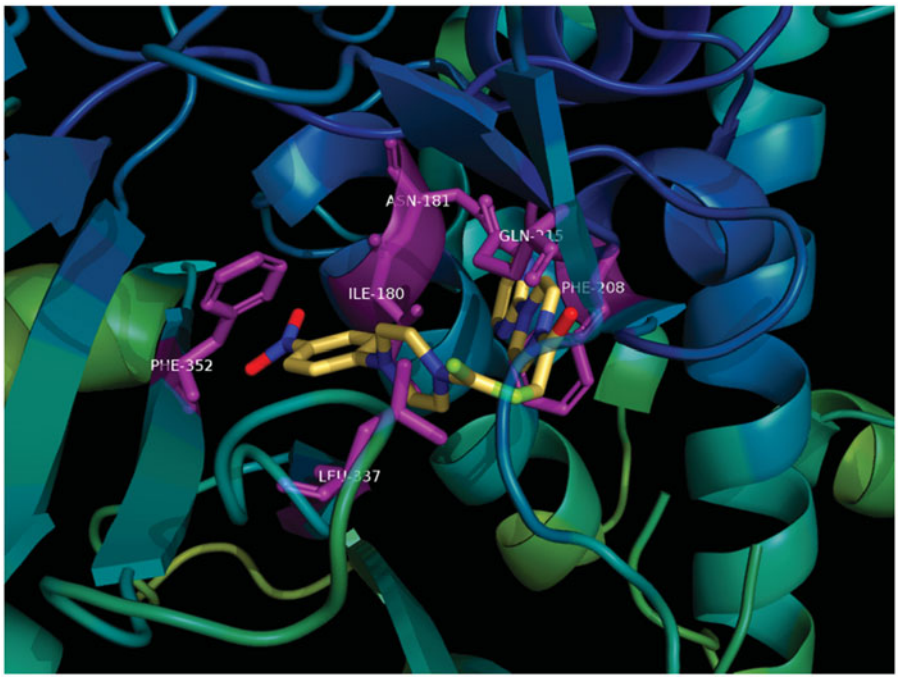

Figure 5. The binding of compound **2j** at the active site of MAO-A enzyme.

inhibitory activities. Compounds **2j** bearing 4-nitrophenyl moiety and **2m** bearing diphenylmethyl moiety has exhibited the highest MAO-A inhibitory activity. Some physicochemical properties and drug-likeness scores of the final compounds (**2a-n**) were also predicted using online Molinspiration and MolSoft programs. The obtained biological data was found to compatible to drug-likeness score (the highest) for compound **2m**. The calculated physicochemical properties were identified in the range determined by Lipinski's rule of five.

Disclosure statement

The authors report no conflict of interest and are responsible for the contents and writing of the paper.

References

1. Blackwell B. Adverse effects of antidepressant drugs. Part 1: monoamine oxidase inhibitors and tricyclics. Drugs 1981;21:201–19.
2. Khattab SN, Abdel-Moneim SAH, Bekhit AA, et al. Exploring new selective 3-benzylquinoxaline-based MAO-A inhibitors: design, synthesis, biological evaluation and docking studies. Eur J Med Chem 2015;93:308–20.
3. Avram S, Buiu C, Duda-Seiman D, et al. Evaluation of the pharmacological descriptors related to the induction of antidepressant activity and its prediction by QSAR/QRAR methods. Mini Rev Med Chem 2012;12:467–76.
4. Shelton RC. Classification of antidepressants and their clinical implications. Prim Care Companion J Clin Psychiatry 2003;5:27–32.
5. Chancellor D. The depression market. Nat Rev Drug Discov 2011;10:809–10.
6. Micó JA, Ardid D, Berrocoso E, et al. Antidepressants and pain. Trends Pharmacol Sci 2006;27:348–54.
7. Millan MJ. The role of monoamines in the actions of established and "novel" antidepressant agents: a critical review. Eur J Pharmacol 2004;500:371–84.
8. Fishback JA, Robson MJ, Xu YT, et al. Sigma receptors: potential targets for a new class of antidepressant drug. Pharmacol Ther 2010;127:271–82.
9. Elmer LW, Bertoni JM. The increasing role of monoamine oxidase type B inhibitors in Parkinson's disease therapy. Expert Opin Pharmacother 2008;9:2759–72.
10. Westlund KN, Denney RM, Rose RM, et al. Localization of distinct monoamine oxidase A and monoamine oxidase B cell populations in human brainstem. Neuroscience 1988;25:439–56.
11. Hall DWR, Logan BW, Parsons GH. Further studies on the inhibition of monoamine oxidase by M & B 9302 (clorgyline), I. Substrate specificity in various mammalian species. Biochem Pharmacol 1969;18:1447–54.
12. Roth JA, Feor K. Deamination of dopamine and its 3-O-methylated derivative by human brain monoamine oxidase. Biochem Pharmacol 1978;27:l606–8.
13. Youdim MB, Finberg JP. New directions in monoamine oxidase A and B selective inhibitors and substrates. Biochem Pharmacol 1991;41:155–62.
14. Youdim MB, Edmondson D, Tipton KF. The therapeutic potential of monoamine oxidase inhibitors. Nat Rev Neurosci 2006;7:295–309.
15. Finberg JPM. Update on the pharmacology of selective inhibitors of MAO-A and MAO-B: focus on modulation of CNS monoamine neurotransmitter release. Pharmacol Ther 2014;143:133–52.
16. Pecknold JC. Serotonin 5-HT1A agonists: a comparative review. CNS Drugs 1994;2:234–51.
17. Bronowska A, Leś A, Mazgajska M, et al. Conformational analysis and pharmacophore design for selected 1-(2-pyrimidinyl)piperazine derivatives with sedative-hypnotic activity. Acta Pol Pharm 2001;58:79–86.
18. Goldberg HL, Finnerty RJ. The comparative efficacy of buspirone and diazepam in the treatment of anxiety. Am J Psychiatry 1979;136:1184–7.
19. Levy AD, Van de Kar LD. Endocrine and receptor pharmacology of serotonergic anxiolytics, antipsychotics and antidepressants. Life Sci 1992;51:83–94.
20. Taylor DP, Moon SL. Buspirone and related compounds as alternative anxiolytics. Neuropeptides 1991;19:15–19.
21. Seidel WF, Cohen SA, Bliwise NG, et al. Buspirone: an anxiolytic without sedative effect. Psychopharmacology (Berl) 1985;87:371–3.
22. Yevich JP, New JS, Lobeck WG, et al. Synthesis and biological characterization of α-(4-fluorophenyl)-4-(5-fluoro-2-pyrimidinyl)-1-piperazinebutanol and analogs as potential atypical antipsychotic agents. J Med Chem 1992;35:4516–25.
23. Chojnacka-Wójcik E, Kłodzińska A, Drabczyńska A, et al. A new putative 5-HT_{1A} receptor antagonist of the 1-arylpiperazine class of ligands. Eur J Med Chem 1995;30:587–92.
24. Ishizumi K, Kojima A, Antoku F. Synthesis and anxiolytic activity of N-substituted cyclic imides (1R*,2S*,3R*,4S*)-N-[4-[4-(2-pyrimidinyl)-1-piperazinyl]butyl]-2,3-bicyclo[2.2.1]heptanedicarboximide (tandospirone) and related compounds. Chem Pharm Bull 1991;39:2288–300.
25. Abou-Gharbia M, Patel UR, Moyer JA, et al. Psychotropic agents: synthesis and antipsychotic activity of substituted beta-carbolines. J Med Chem 1987;30:1100–5.
26. Abou-Gharbia M, Moyer JA, Patel U, et al. Synthesis and structure-activity relationship of substituted tetrahydro- and hexahydro-1,2-benzisothiazol-3-one 1,1-dioxides and thiadiazinones: potential anxiolytic agents. J Med Chem 1989;32:1024–33.
27. Taylor DI, Hyslop DK, Riblet LA. Trazodone, a new nontricyclic antidepressant without anticholinergic activity. Biochem Pharmacol 1980;29:2149–50.
28. Becker I. Preparation of derivatives of 1-(2-pyrimidinyl)piperazine as potential antianxiety, antidepressant, and antipsychotic agents. J Heterocyclic Chem 2008;45:1005–22.
29. Prashanth MK, Revanasiddappa HD, Lokanatha Rai KM, et al. Synthesis, characterization, antidepressant and antioxidant activity of novel piperamides bearing piperidine and piperazine analogues. Bioorg Med Chem Lett 2012;22:7065–70.
30. Gomółka A, Ciesielska A, Wróbel MZ, et al. Novel 4-aryl-pyrido[1,2-c]pyrimidines with dual SSRI and 5-HT1A activity. Part 5. Eur J Med Chem 2015;98:221–36.
31. Matsumoto T, Suzuki O, Furuta T, et al. A sensitive fluorometric assay for serum monoamine oxidase with kynuramine as substrate. Clin Biochem 1985;18:126–9.
32. Küçükgüzel SG, Küçükgüzel İ, Tatar E, et al. Synthesis of some novel heterocyclic compounds derived from diflunisal hydrazide as potential anti-infective and anti-inflammatory agents. Eur J Med Chem 2007;42:893–901.
33. http://www.molinspiration.com/cgi-bin/properties [last accessed 25 Oct 2016].
34. http://molsoft.com/mprop/Last [last accessed 25 Oct 2016].

35. Zhao Y, Abraham MH, Lee J, et al. Rate-limited steps of human oral absorption and QSAR studies. Pharm Res 2002;19:1446–57.
36. Bakht MA, Yar MS, Abdel-Hamid SG, et al. Molecular properties prediction, synthesis and antimicrobial activity of some newer oxadiazole derivatives. Eur J Med Chem 2010;45:5862–9.
37. Lipinski CA, Lombardo F, Dominy BW, et al. Experimental and computational approaches to estimate solubility and permeability in drug discovery and development settings. Adv Drug Deliv Rev 1997;23:3–25.
38. Kaya B, Sağlık BN, Levent S, et al. Synthesis of some novel 2-substituted benzothiazole derivatives containing benzylamine moiety as monoamine oxidase inhibitory agents. J Enzym Inhib Med Chem, Article in press.
39. Trott O, Olson AJ. AutoDock Vina: improving the speed and accuracy of docking with a new scoring function, efficient optimization, and multithreading. J Comput Chem 2010;31:455–61.
40. Sanner MF. Python: a programming language for software integration and development. J Mol Graph Model 1999;17:57–61.
41. The PyMOL Molecular Graphics System, Version 1.8, Schrödinger, LLC.
42. Abdelhafez OM, Amin KM, Ali HI, et al. Monoamine oxidase A and B inhibiting effect and molecular modeling of some synthesized coumarin derivatives. Neurochem Int 2013;62:198–209.
43. Yurttaş L, Özkay Y, Duran M, et al. Synthesis and antimicrobial activity evaluation of new dithiocarbamate derivatives bearing thiazole/benzothiazole rings. Phosphorus Sulfur Silicon Relat Elem 2016;191:1166–73.